

Supplementary Methods

Cell culture and gene transfection

Cells were cultured in RPMI1640 medium (Invitrogen) with 10% FBS and 50 µg/ml gentamycin. Cells were grown in 75 cm² culture flasks or 60 mm² dishes at 37°C in humidity with 5% (v/v) CO₂. Media were changed every two days. For establishment of stable clones that expressed Flag and Flag-HOXB13 separately, H1299 cells were transfected with Flag-HOXB13 and Flag, and A549 were transfected with GFP-HOXB13 and GFP using Lipofectamine. Twenty-four hours after transfection cells were passaged and G418 was added at final concentration of 1200 µg/ml (H1299) and 800 µg/ml (A549) separately. H1299 and A549 cells were transfected with HOXB13 siRNA and control siRNA using RNAiMAX. Sequences of RNA interference (RNAi) oligonucleotides used for knocking down of endogenous HOXB13 were designed as shown in Supplementary Methods.

Western blot analysis

PBS/TDS lysis buffer with the presence of protease cocktail inhibitor (Roche Diagnostics, GmbH) was used to extract total cell lysates. Added 20 % of 5× SDS loading buffer into 80 % of cell lysates then resolved by 10% SDS-PAGE gel and blotted onto PVDF membranes (pore size 0.45 µm). The primary antibodies: HOXB13 mouse monoclonal antibody (Milipore, USA) 1:1000, E-cadherin rabbit monoclonal antibody (Epitomics, USA) 1:1000, Vimentin mouse monoclonal antibody (Santa Cruz, USA) 1:1000, EZH2 mouse monoclonal (Santa Cruz, USA) 1:1000, ABCG1 mouse monoclonal antibody (Santa Cruz, USA) 1:1000, Flag Clone M2 mouse monoclonal antibody (Sigma, USA) 1:10000, GFP rabbit polyclonal antibody (Abcam, USA) 1:1000, MMP-2 mouse monoclonal antibody (Epitomics, USA) 1:1000, MMP-3 mouse

monoclonal antibody (Epitomics, USA) 1:1000, MMP-9 mouse monoclonal antibody (Epitomics, USA) 1:1000, and N-cadherin mouse monoclonal antibody (Sigma, USA) 1:1000 were incubated separately with the membranes under rotation. After thorough washing, membranes were further incubated with corresponding secondary antibodies recognizing either rabbit or mouse Ig (Jackson Laboratories, USA). Finally, the bands were visualized by the enhanced chemoluminescence (Pierce).

Sequences of RNA interference (RNAi) oligonucleotides

Control siRNA: UUCUCCGAACGUGUCACG, HOXB13 siRNA1:

CAAAGUAACCAUAAGGCACGGGAGC, HOXB13 siRNA2:

UGAUGAACUUGUUAGCCGCAUACUC, EZH2 siRNA1: GACTCTGAATGCAGTTGCT,

EZH2 siRNA2 GCAAATTCTCGGTGTCAAA,

ABCG1 siRNA1: GACUAGUGUACAAAUCCGGGCAGAGA, ABCG1 siRNA2:

CGUGGAUGAGGUUGAGACA, Slug siRNA1: CAAGAAGCAUUUCAACGCCUCCAAA,

Slug siRNA2: GCAUUUGCAGACAGGUCAA

Quantitative polymerase chain reaction (qPCR)

Quantitative PCR assays were performed to detect the expression of HOXB13, ABCG1, EZH2 mRNA in H1299 Flag-HOXB13 and A549 siHOXB13 controlled with H1299 Flag and A549 si-control respectively. In brief, total cellular mRNAs were isolated by Trizol (Invitrogen, CA, USA), and 2 µg of total RNA was reverse transcribed using M-MLV reverse transcriptase (Promega, CA, USA). Then PCR was performed using Taq PCR MasterMix (TIANGEN, China) with the settings as: 94°C 2 min; 94°C 30 sec, 60°C 30 sec, 72°C 30 sec, for 30 cycles; 72°C 5

min. The primers for qPCR were designed: HOXB13-F GTGCTGCCCCGCTGGAGTC, HOXB13-R AGTTACCTGGACGTGTCTGTGG; Slug-F AGA TGCATATTCGGACCCAC, Slug-R CCTCATGTTTGTGCAGGAGA; ABCG1-F GGAGAATGCGAAGCTG TACC, ABCG1-R GGAGGCGGTTTTTACCTCTC; EZH2-F TTGTTGGCGGAA GCGTGTA AAAATC, EZH2-R TCCCTAGTCCC GCGCAATGAGC; Actin-F CTGAG CGTGGCTACTCCTTC, Actin-R GCCATCTCGTTCTCGAAGTC. Relative fold changes in qPCR were determined by the $\Delta\Delta C_t$ method.

ChIP assay

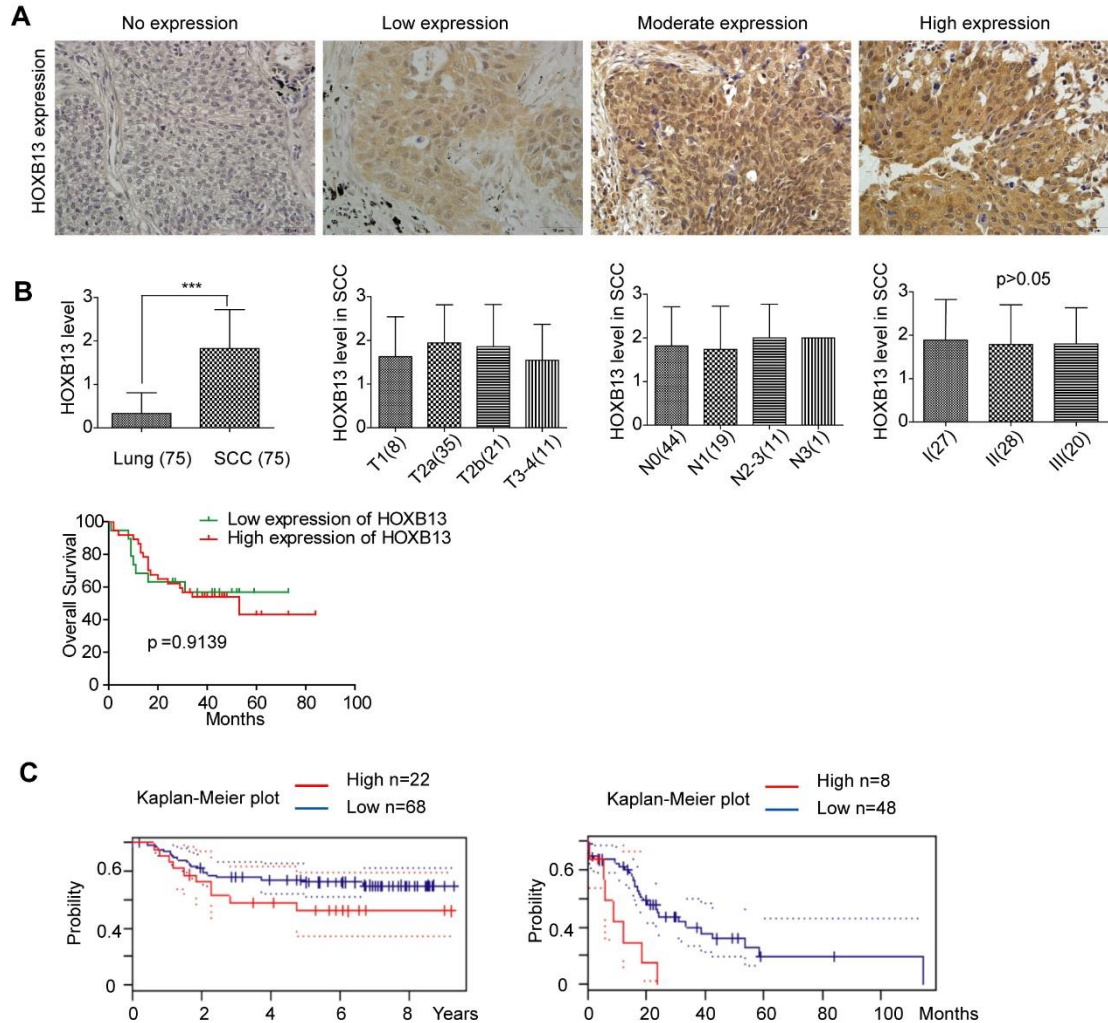
Chromatin immunoprecipitation assays were performed using Magna ChIP™ A/G Chromatin Immunoprecipitation Kit (catalog#17-10085, Millipore) as described. Briefly, H1299 cells stably expressing Flag-HOXB13 were cross-linked in 1 % formaldehyde at room temperature for 10 min. The reaction was quenched with 0.125 M glycine at room temperature for 5 min. After washed twice with cold PBS, cells were collected and suspended in cell lysis buffer with protease inhibitor Cocktail II (Sigma) to isolate nuclei. Then the pellet of nuclei was suspended in the nuclear lysis buffer containing Cocktail. The nuclear extracts were sonicated to obtain DNA fragments with an average size of 300-500 bp. After centrifugation, the supernatant, diluted with dilution buffer, was immunoprecipitated with the HOXB13 antibody (SC-28333x, Santa Cruz, USA) or control normal mouse IgG. The complex was precipitated with protein A/G magnetic beads overnight. Washed with low salt wash buffer, high salt wash buffer, LiCl wash buffer and TE buffer, the magnetic beads were eluted in elution buffer with protease K at 62°C for 2 h to reverse cross-links. DNA fragments were purified with the spin filter and analyzed by real-time PCR with primers: EZH2-1600 Forward: TGCCACATGAAGCAATAGGA, Reverse:

CAGAGCGAGACTCCATCTCA, EZH2-1400 Forward: CCCGAGTAGCTG GGA CTACA,
Reverse: GATCGAGACCATCCTGGCTA, EZH2-1100 Forward:
GGCAGCAGCAGACATAATCA, Reverse: GTCAGGCTGGTCTCGAACTC, EZH2-800
Forward: TAATCCAGCTACTCGGGAGG, Reverse: GAGTTTCGCTC TGGTTGTCC, EZH2-
500 Forward: CTGGTTCAA ACTTGGCTTCC, Reverse: GTTCTTTCGCTGAACACACG,
EZH2-200 Forward: GCGTCCCTTACAGCGAAC; Reverse: ATCGCCATCGCTTTTATTTG,
Slug-2900 Forward: GGCTGGCCCAG ATCTTTAAC, Reverse:
CACCCCAGACACCCGTATAA, Slug-2700 Forward: ATGGCCTCCAGAGTTCCTTT,
Reverse: TTAGAGCCACGTGGACACAG, Slug-2500: Forward:
GCTGATAAACCCAATCAGCC Reverse: ATGGAACAA GCAAACCCAAG, Slug-2300
Forward: GCAGTTGCCTCCACAAAGAT, Reverse: ATGTGGTAAAAACGCAAGCC, Slug-
2100 Forward: TGTCTGAGCAGAGCA CCTGT, Reverse: AGCGAGTAACACGTATGCCC,
Slug-1000 Forward: AGGA AATCTGTGAGTGCCCC, Reverse:
TCACATGAAGATCACCTACTCT, Slug-500 Forward: TGAGAGAATGTCCGGTGGTT,
Reverse: ACTCATGTCACCGTGT TAGC, NKX3.1-promoter Forward:
ACAGGGTGGCCCAAATAGAAC, Reverse: CCTGTCTTGGACAAGCGGAGA, ORM1-
promoter Forward: GGGTCATT TCCACCACCTCAAACA, Reverse:
GGAGAAAGGCCTTACAGTAGTCTC, ABCG1-promoter Forward:
TCTGTGCCTTACTTCCCCAC, Reverse: GAAA GTGAGCTGGTGAAGCC, HOXB13-
promoter Forward: CATCTGGGACA GGAAGGGTA, Reverse:
GCCTGTGTAAGAGGAGGCTG, Actin-promoter Forward: CACCAGGTAGGGGAGCTG,
Reverse: GAAAGGACAAGAA GCCCTGAG.

Primers used in luciferase reporter assay

The primers used to clone the promoter into the pGL4.21 vector were used. pGL4.21-ABCG1-1000 Forward: CCCCTCGAGGCATGAATCACAAAAACA, pGL4.21 ABCG1 750 Forward: CCCCTCGAGACAGAAAGATTTGTGCAC, pGL4.21 ABCG1 500 Forward: CCCCTCGAGTTCATTCCATTCGTCCTT, pGL4.21 ABCG1 265 Forward: CCCCTCGAGTAAAAATAAATTCCACT, pGL4.21 ABCG1 Reverse: CCGAAGCTTCACTGCAGGCATGTAAAG, ABCG1 265 Reverse: GATTGCCAAGCTTGGTGGTTCAGCGCGCC, pGL4.21 EZH2 1875 Forward: CCGCTCGAGAGATTTTTACCCCAACAG, pGL4.21 EZH2 1062 Forward: CCGCTCGAGGGCCGAGGCGGGCGGATC, pGL4.21 EZH2 612 Forward: CCGCTCGAGACTTGGCTTCCAGCACCC, pGL4.21 EZH2 Reverse: CCCAAGCTTCACTGCCTTCTGAGTCCC, pGL4.21 HOXB13 810 Forward: CCGCTCGAGTAGGGAGAGGACTGCAGG, pGL4.21 HOXB13 660 Forward: CCGCTCGAGCTCTTCTTTCTCTTTTCT, pGL4.21 HOXB13 229 Forward: CCGCTCGAGGGTACCGGGAATGAACTG, pGL4.21 HOXB13 Reverse: CCCAAGCTTCTTGGCTCCATCCAAGGT.

Supplementary Figure 1.

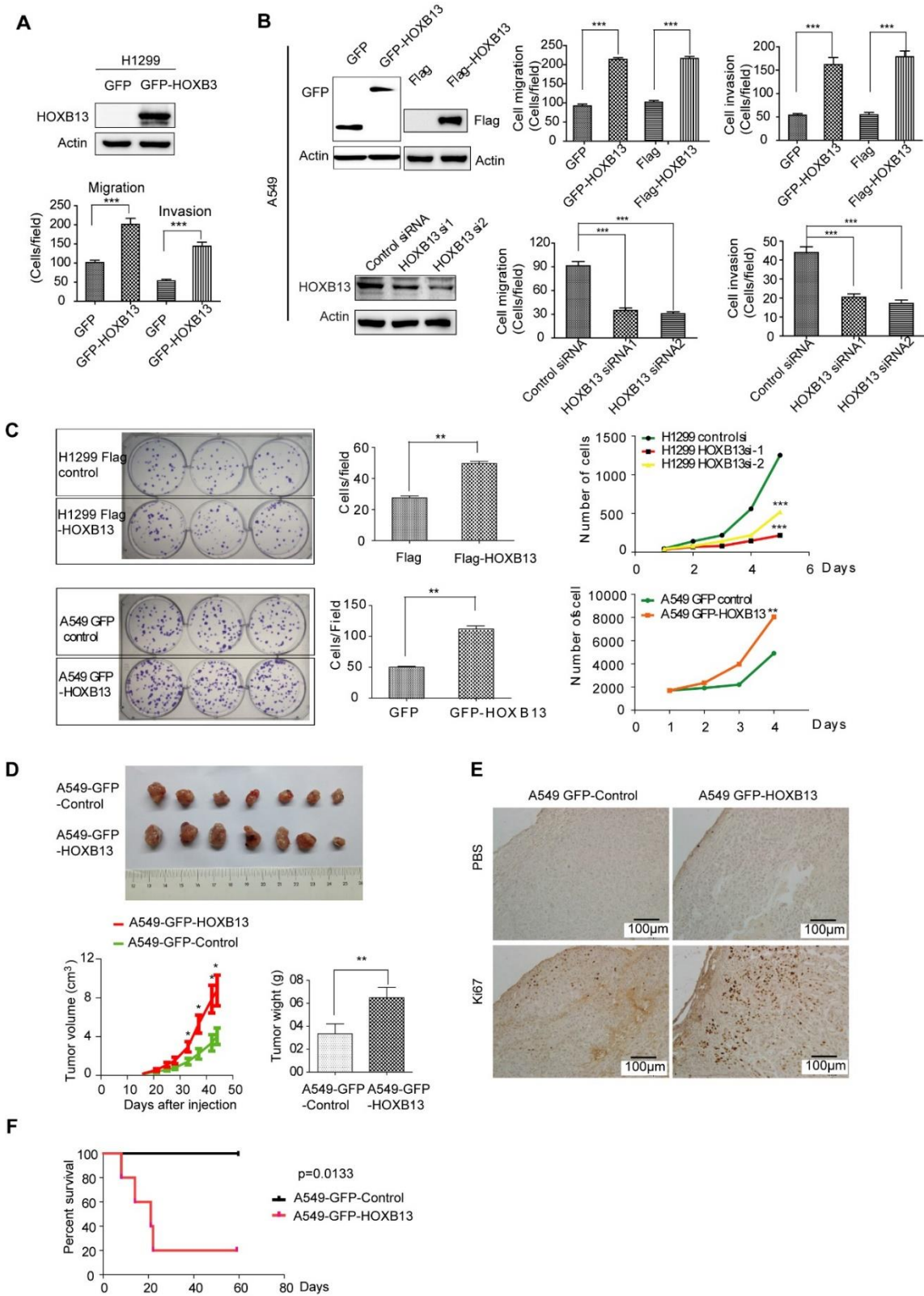


Supplementary Figure 1. Clinicopathological significance of HOXB13 in SCC. (A)

Expression of HOXB13 in SCC. (B) Semi-quantitative analysis of HOXB13 levels in SCC patients. The expression level of HOXB13 is significantly higher in SCC tissue than in normal lung tissue ($p < 0.01$). No obvious correlation between HOXB13 expression level and T grade, N grade and AJCC grade in SCC (One-way ANOVA analysis, $p > 0.05$). And HOXB13 expression is not correlated with overall survival in SCC patients (Kaplan-Meier analysis, with log-rank at $p = 0.9139$). (C) After re-analyzing the relative datasets we supplemented two more results to support the observation of a strong correlation between elevated levels of HOXB13 and clinical

outcomes of the patients with lung cancer, which further supported our findings. Left: In GSE14814 dataset, 90 cases of NSCLC frozen samples were analyzed and a relationship between HOXB13 mRNA level and the disease specific survival was established. The Cox p-value is 0.028434, HR=2.24 (1.09-4.8). Right: In GSE17710 dataset, 56 cases of SCC frozen samples were analyzed and a relationship between HOXB13 mRNA level and the relapse free survival was established. The corrected p-value is 0.049894, HR=2.33 (0.92-1.9).

Supplementary Figure 2.



Supplementary Figure 2. HOXB13 promotes lung cancer cell migration, invasion and

growth in vitro and in vivo. (A) GFP-HOXB13 promoted H1299 cell migration and invasion.

(B) HOXB13 promoted A549 cell migration and invasion. Upper panel left: GFP-HOXB13 and Flag-HOXB13 was stably transfected in A549 cells controlled by GFP and Flag empty vector respectively. Upper panel middle: HOXB13 effect on cell migration was determined in a

Transwell assay. Upper panel right: HOXB13 effect on cell invasion on Matrigel was examined using A549 cells stably expressing GFP-HOXB13 and Flag-HOXB13. Lower panel left: Western blot showed that HOXB13 were knocked down by two HOXB13 siRNAs in A549 cells. Lower

panel middle: A549 cell migration was measured in a Transwell assay after HOXB13 depletion.

Lower panel right: A549 cell invasion on Matrigel was measured using Transwell after HOXB13

depletion. (C) HOXB13 promoted lung adenocarcinoma cell proliferation. Left panel: Plate colony formation experiment was performed to measure the role of HOXB13 in promoting

proliferation by overexpression of HOXB13. Middle panel: Quantification of the plate colony formation experiment in left panel. Data were expressed as mean \pm SEM from three repeating

experiments (Students' *t* test, ** $p < 0.01$). Right panel: HOXB13 is required for H1299 cell

growth. H1299 cells were transiently transfected with two HOXB13 siRNAs separately and

controlled by scramble siRNA. A549 cells transiently transfected with GFP-HOXB13, controlled by GFP empty vector. Cell growth was measured by counting the cell numbers at indicated days.

Data were expressed as mean \pm SEM from three repeating experiments (Students' *t* test,

** $p < 0.01$, *** $p < 0.01$). (D) HOXB13 promotes tumor formation in A549 cells. 1×10^6 A549 cells

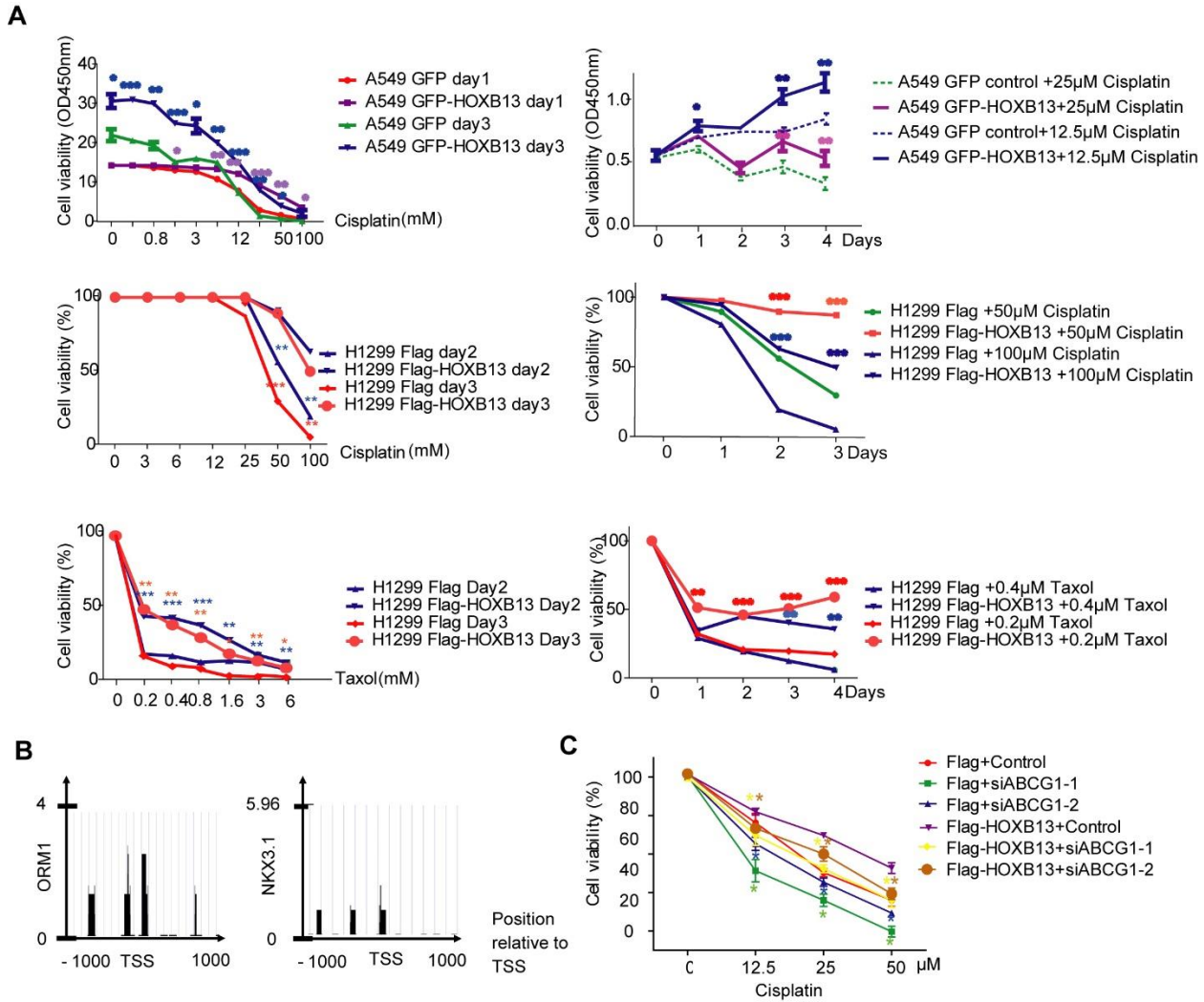
stably expressing GFP-HOXB13 or control vector were inoculated into the flank of nude mice.

At day 28, tumors were dissected and photographed. The mice were continued to be fed until the

day 56 and the survival information was recorded. Upper panel: Tumor formation photos. Lower

panel left: Tumor growth curve for GFP-HOXB13-A549 and control cells. lower panel right: Average weights of tumor at the end-point. (E) Proliferation marker Ki67 was detected by IHC in tumor tissue expressing GFP-HOXB13 compared with those stably expressing GFP. (F) Nude mice with or without stable expression of GFP-HOXB13 were determined by Kaplan-Meier analysis and showed that elevated expression of HOXB13 in tumor cells correlates to poor overall survival for xenografted nude mice (log-rank at $p=0.00133$).

Supplementary Figure 3.



Supplementary Figure 3. ABCG1 mediates HOXB13-induced multidrug resistance in lung

adenocarcinoma cells in vitro. (A) High expression of HOXB13 induces multidrug resistance

in lung adenocarcinoma cells in vitro by WST-1 cell viability assay detection. Upper panel left:

Enhanced expression of HOXB13 promotes A549 cell resistance to cisplatin. Upper panel right:

Time course of cisplatin effects on A549 GFP control and A549 GFP-HOXB13 cells. Middle

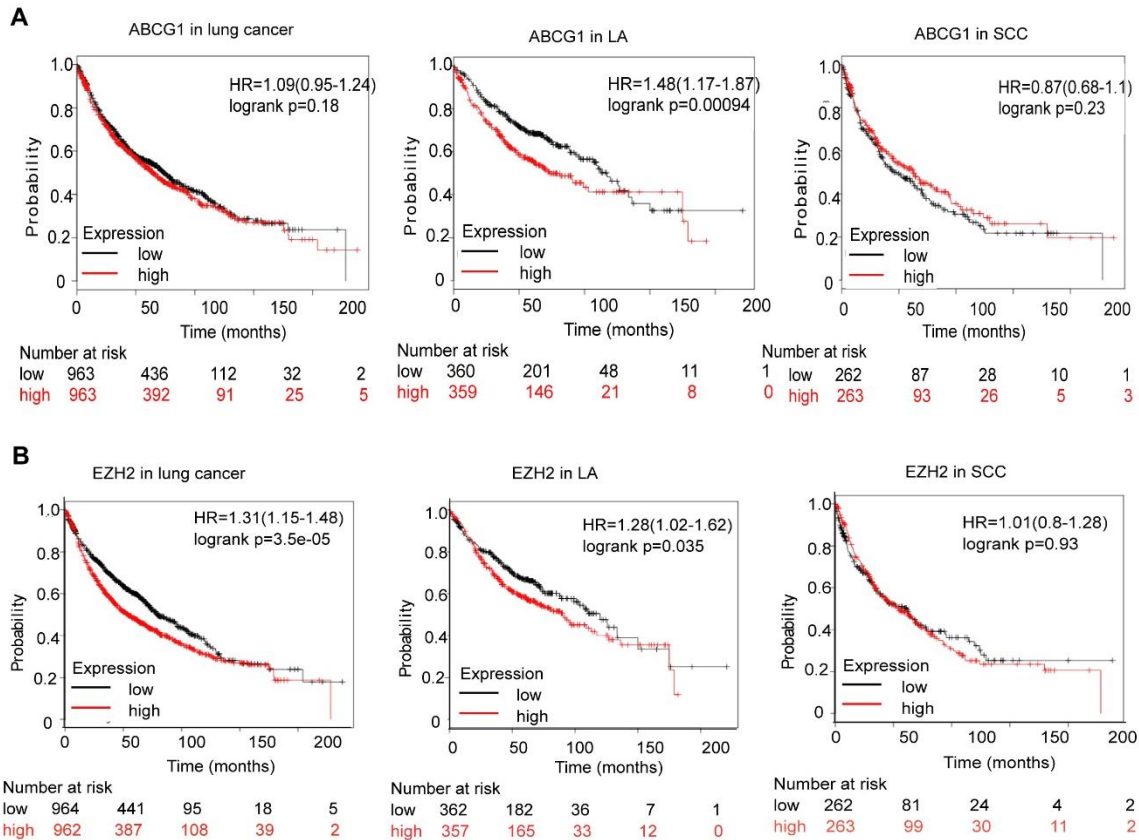
panel left: Increased expression of HOXB13 promotes H1299 cell resistance to cisplatin. Middle

panel right: Time course of cisplatin effects on H1299 Flag and H1299 Flag-HOXB13 cells.

Lower panel left: Increased expression of HOXB13 promotes H1299 cell resistance to paclitaxel.

Lower panel right: Time course of paclitaxel effects on H1299 Flag and H1299 Flag-HOXB13 cells. Different color stars indicate the significant increase of cell viability curve with the same color compared with the respective control cells at the indicated concentration of drugs or at the indicated time points (* $p < 0.05$, ** $p < 0.01$ and *** $p < 0.001$). (B) Enrichment of HOXB13 on the ORM1 and NKX3.1 promoter analyzed by ChIP-seq database from prostate cancer. (C) ABCG1 mediates HOXB13 induced cisplatin resistance in A549 cells. Depletion of ABCG1 enhanced drug sensitivity of A549 cells to cisplatin with/without HOXB13 overexpression. Cells were treated with various doses of cisplatin for 48 h. The stars of different colors represent a significant difference in the corresponding curve of the color compared with the according control cells (* $p < 0.05$, ** $p < 0.01$).

Supplementary Figure 4.

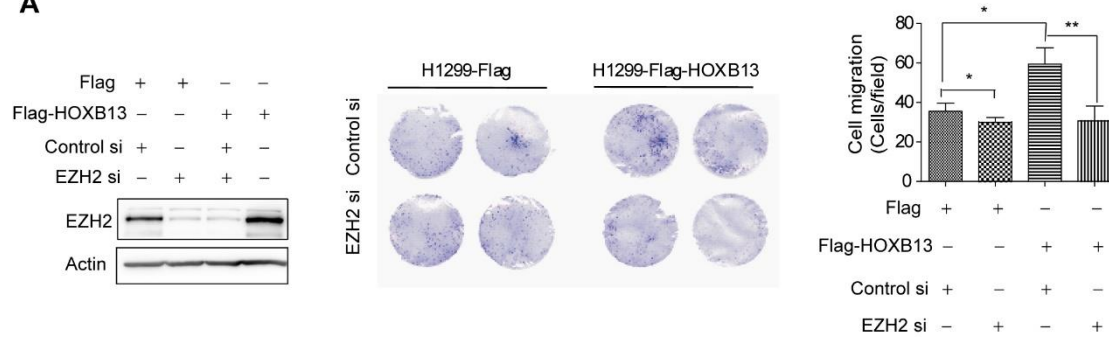


Supplementary Figure 4. High expression of ABCG1 and EZH2 predicts poor outcome in lung adenocarcinoma patients by K-M plot analysis.

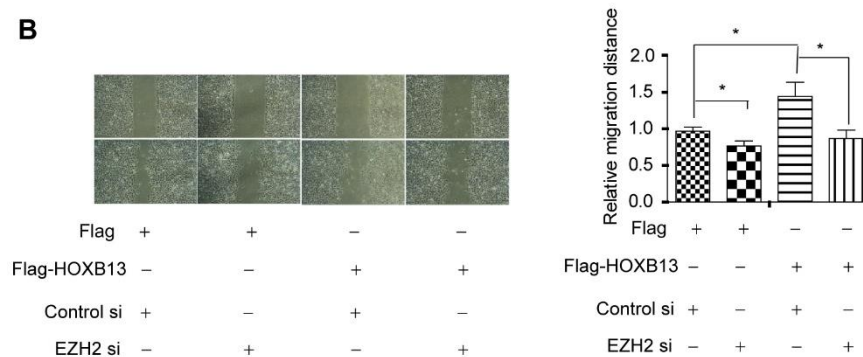
(A) High expression of ABCG1 predicts poor outcome in lung adenocarcinoma patients by K-M plot analysis. Left: Correlation of ABCG1 gene expression level with OS in 1926 lung cancer patients ($p=0.18$). Middle: Correlation of ABCG1 gene expression level with OS in 719 cases of lung adenocarcinoma patients ($p=0.00094$). Right: Correlation of ABCG1 gene expression level with OS in 525 cases of SCC patients ($p=0.23$). (B) High expression of EZH2 predicts poor outcome in lung adenocarcinoma patients by K-M plot analysis. Left: In 1,926 patients with lung cancer ($p=3.5 \times 10^{-5}$). Middle: In 719 cases with lung adenocarcinoma ($p=0.035$). Right: In 525 cases of SCC ($p = 0.93$).

Supplementary Figure 5.

A



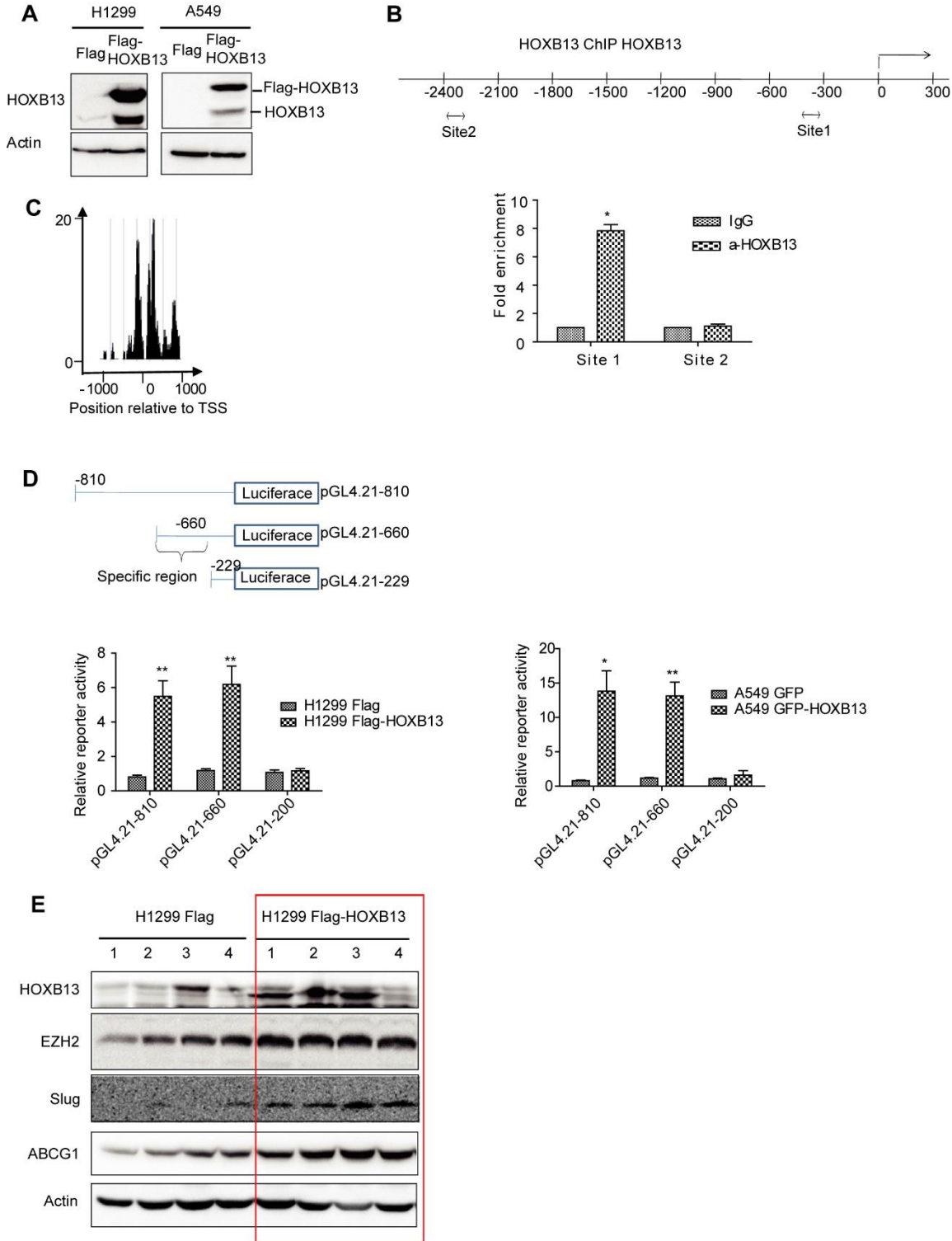
B



Supplementary Figure 5. HOXB13-enhanced H1299 cell migratory ability is jeopardized

by EZH2 depletion. (A) H1299 cells stably expressing Flag-HOXB13 were transfected with EZH2 siRNA, control cells and siRNA were indicated. Left: EZH2 depletion was detected by Western blot analysis. Middle: Transwell assay were adopted to detect the migratory ability of indicated cells. Right: Quantification of cell migration ability in Transwell assay (* $p < 0.05$, ** $p < 0.01$). (B) Left: Wound healing assay were adopted to detect the migratory ability of indicated cells. Right: Quantification of cell migratory ability in wound healing assay (* $p < 0.05$).

Supplementary Figure 6.



Supplementary Figure 6. HOXB13 targets to its own promoter and constitutes a positive feedback loop in lung adenocarcinoma cells. (A) H1299 and A549 lung adenocarcinoma cells

were transiently transfected with Flag-HOXB13 separately. Cell lysates were made and separated by 15% SDS-PAGE gel. Western blot analysis was performed using an anti-HOXB13 antibody. Endogenous and exogenous HOXB13 were indicated. (B) HOXB13 targets to its own promoter

Upper panel: Potential HOXB13 binding region was shown in the HOXB13 promoter (double arrow). Lower panel: ChIP analysis was performed using either an anti-HOXB13 ChIP grade antibody or control IgG in H1299 Flag-HOXB13 cells and Site 1 was found enriched under HOXB13 overexpression as determined by qPCR analysis. Already known HOXB13 target genes ORM1, NKX3.1 were used as positive controls, and actin was used as a negative control.

(C) Enrichment of HOXB13 on HOXB13 promoter analyzed by ChIP-seq from prostate cancer database. (D) Luciferase reporter assay to identify the specific region of HOXB13 targeting on its own promoter. Upper panel: HOXB13 promoter-luciferase reporter construct map. Lower panel left: Luciferase activity of each construct co-transfected with vector or HOXB13, towards the identification of a 200-660bp upstream region critical for HOXB13-directed enhancement (* $p < 0.05$, ** $p < 0.01$) in H1299 cells. Lower panel right: Luciferase activity in A549 cells. (E) HOXB13 targeting proteins EZH2, Slug, HOXB13 and ABCG1 were all induced in H1299 Flag-HOXB13 xenografted tumor tissues. Tumor tissue lysates were prepared and were subjected to Western blot analysis with indicated antibodies.